9518 *Biochemistry* **2010,** *49,* 9518–9532
DOI: 10.1021/bi1009584

BIOCHEMISTRY
including biophysical chemistry & molecular biology
Article

Monovalent Interactions of Galectin-1[†]

Emma Salomonsson,[‡] Amaia Larumbe,[§] Johan Tejler,[§] Erik Tullberg,[§] Hanna Rydberg,[‡] Anders Sundin,[§] Areej Khabut,[‡] Torbjörn Frejd,[§] Yuri D. Lobsanov,[∥] James M. Rini,[⊥] Ulf J. Nilsson,[§] and Hakon Leffler*[,‡]

[‡]*Section MIG, Institute of Laboratory Medicine, Lund University, Sölvegatan 23, SE-223 62 Lund, Sweden,* [§]*Organic Chemistry, Lund University, P.O. Box 124, SE-221 00 Lund, Sweden,* [∥]*Molecular Structure and Function Research Institute, Hospital for Sick Children, 555 University Avenue, Toronto, Ontario, M5G 1X8 Canada, and* [⊥]*Departments of Molecular Genetics and Biochemistry, University of Toronto, Toronto, Ontario, M5S 1A8 Canada*

Received June 14, 2010; Revised Manuscript Received September 26, 2010

ABSTRACT: Galectin-1, a β-galactoside binding lectin involved in immunoregulation and cancer, binds natural and many synthetic multivalent glycoconjugates with an apparent glycoside cluster effect, that is, affinity above and beyond what would be expected from the concentration of the determinant sugar. Here we have analyzed the mechanism of such cluster effects in solution at physiological concentration using a fluorescence anisotropy assay with a novel fluorescent high-affinity galectin-1 binding probe. The interaction of native dimeric and monomeric mutants of rat and human galectin-1 with mono- and divalent small molecules, fetuin, asialofetuin, and human serum glycoproteins was analyzed. Surprisingly, high-affinity binding did not depend much on the dimeric state of galectin-1 and thus is due mainly to monomeric interactions of a single carbohydrate recognition domain. The mechanism for this is unknown, but one possibility includes additional interactions that high-affinity ligands make with an extended binding site on the carbohydrate recognition domain. It follows that such weak additional interactions must be important for the biological function of galectin-1 and also for the design of galectin-1 inhibitors.

Galectin-1 is a member of a family of small soluble carbohydrate binding proteins, which are attracting increasing attention as, e.g., modulators of the immune system and of cancer progression (*1*, *2*). The basic cellular function of galectin-1 is not known, but one emerging role, as for other galectins, is the formation of microdomains (lattices) within membranes (*3*−*5*) that in turn affect intracellular trafficking and cell surface presentation of glycoprotein receptors (*6*−*10*). These effects require cross-linking of ligands by the dimeric galectin-1, and many ligands are also bound with an apparent "glycoside cluster effect", that is, affinity above and beyond what would be expected from the concentration of the determinant sugar (*11*, *12*) (*13*) (*14*), as for many other carbohydrate binding proteins (*15*, *16*).

The immunomodulatory effects of galectin-1, resulting from the cross-linking described above, include immunosuppression and shifting the Th1/Th2 balance by various mechanisms, such as selective induction of apoptosis in Th1 cells (*17*), or induction of selected interleukin secretion (*18*). The immunosuppressive effect can promote cancer by antagonizing anticancer T-cells (*2*), but galectin-1 can also promote cancer via angiogenesis (*19*) or cell migration (*20*). Because of these roles, galectin-1 is itself a potential immunosuppressive therapeutic (*21*) and a potential target for the development of inhibitors to be used as immunomodulatory and anticancer agents (*2*). Multivalent lactose derivatives designed as inhibitors (*4*, *22*−*27*) have shown an apparent "glycoside cluster effect" (*14*). From this follows an interest in understanding how galectin-1 works. A better definition of the relationship between its cross-linking ability and its affinity would provide a better understanding of its function in cells and also guide the development of inhibitors. Are multivalent inhibitors an advantage as proposed for many other carbohydrate binding proteins (*15*, *16*, *23*), or does design of monovalent inhibitors provide a better alternative?

Galectin-1 is a homodimer (*28*) of the typical galectin carbohydrate recognition domain (CRD), a domain defined by affinity for β-galactose and a conserved amino acid sequence motif (*29*). Most of the biological activities of galectin-1 require the dimeric form, as they are not seen with monovalent mutants (*13*). However, biological function also depends on the detailed binding specificity of the CRD itself. The ∼135 amino acid galectin CRD has a carbohydrate binding groove, long enough to accommodate a tetrasaccharide, and therefore, for convenience, labeled by site A, B, C, and D (*29*) (Figure 1); C is the defining galactose binding site formed by the conserved amino acid motif, while the other sites vary among galectins and give each its different specificity for a subset of β-galactosides. In the N-glycans of common mammalian glycoproteins, both galectin-1 and -3 typically bind a terminal LacNAc moiety in site C−D, and for both galectins binding is blocked by the addition of NeuAcα2−6 (to the Gal) which sits in site B. Addition of NeuAcα2−6 to the Gal is thought to make Th2 lymphocytes resistant to galectin-1-induced apoptosis and thereby govern its regulation of the Th1/Th2 balance, but it does not make Th2 cells resistant to galectin-3 (*17*). Therefore, there must be additional determinants of this galectin function.

The properties of galectin-1 described above raise the question of how the relatively complex binding sites of each CRD cooperate to achieve ligand binding affinity, cross-linking, and

[†]Funding was from the Lund University Research School in Pharmaceutical Sciences, the Swedish Research Council, the programs "Glycoconjugates in Biological Systems" and "Chemistry for the Life Sciences" sponsored by the Swedish Strategic Research Foundation, and the Royal Physiographic Society in Lund.

*To whom correspondence should be addressed. Tel: (46) 46 173270. Fax: (46) 46 137468. E-mail: Hakon.Leffler@med.lu.se.

 Published on Web 09/28/2010

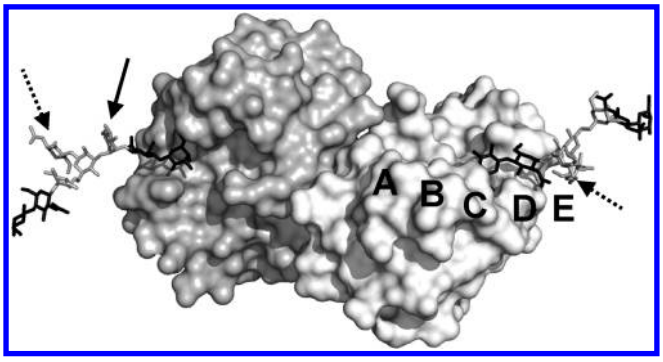

FIGURE 1: Structure of homodimeric galectin-1. The two CRDs are shown as surfaces, each binding to a N-glycan, shown as a stick model. The subsites of the galectin carbohydrate binding site are labeled A−E. The LacNAc residues, two for each N-glycan, are in black, and the trimannosyl core and one of the two core GlcNAc-residues are in gray. The dotted arrows point to the latter, where the saccharide would be linked, via one more GlcNAc residue, to an asparagine side chain in a glycoprotein. The unbroken arrow points to the position of a Man residue where an additional antenna would be attached. One LacNAc from each N-glycan is in the canonical galectin binding site (C−D). The model was built based on PDB coordinates 1SLA from ref *45* using PyMOL, DeLano Scientific LLC.

biological function. Here we have addressed the role of galectin-1 oligomerization by analyzing the interaction of monomeric and dimeric galectin-1 with a number of monovalent, divalent, or multivalent ligands in solution at physiological concentrations. This has been made possible using a fluorescence anisotropy assay (FA assay)[1] with a newly designed fluorescent probe with high affinity for galectin-1. Surprisingly, the results show that dimeric galectin-1 is not required for high-affinity ligand binding but rather that high-affinity binding may arise from extended ligand interactions with a single CRD.

EXPERIMENTAL PROCEDURES

Galectins. Clones expressing human galectin-1 (dHumGal-1w) and a mutant monomeric form (C3S/V6D; mHumGal-1) were kind gifts from Professor Richard Cummings, Department of Biochemistry, Emory School of Medicine, Atlanta, GA (*30*), and a clone expressing human galectin-1 C3S (dHumGal-1) was a kind gift from Dr. Jun Hirabayashi, Research Center for Glycoscience, National Institute of Advanced Industrial Science and Technology (AIST), Tsukuba, Japan (*31*). Rat galectin-1 (dRatGal-1w) (*32*) was mutated to a monomeric form (mRatGal-1) by introducing the substitutions corresponding to those in the monomeric form of human galectin-1. An additional mutant of human galectin-1 C3S was also made, by introducing an Asp instead of an Asn in position 34 (dHumGal-1, C3S/N34D). Mutants were generated using the QuickChange II site-directed mutagenesis kit (Stratagene). Template DNA was isolated from *Escherichia coli* XL1Blue (Stratagene). Mutagenic primers for PCR were as follows: (mRatGal-1) sense (5′-gga gat acc atg gcc tct ggt ctg gac gcc agc aac-3′) and antisense (5′-gtt gct ggc gtc cag acc aga ggc cat ggt atc tcc-3′) and (dHumGal-1, C3S/N34D) sense (5′-cta aga gct tcg tgc tgg atc tgg gca aag aca gc-3′) and antisense (5′-gct gtc ttt gcc cag atc cag cac gaa gct ctt ag-3′). Successful mutagenesis was confirmed by sequencing in the forward direction from the T7 promoter primer. Recombinant proteins were produced and purified by affinity chromatography on lactosyl-Sepharose essentially as described (*32*), including elution with water as described before for rat galectin-1 (*32*).

Dynamic Light Scattering. Particle size of monomeric and dimeric human galectin-1 was measured by dynamic light scattering (DLS) using a Malvern Instruments Zetasizer Nano-S instrument (Malvern Instruments Ltd., Worcestershire, U.K.). For measurement, different concentrations of protein (ranging from 5 to 160 μM) were prepared in PBS. Aggregation of asialofetuin (ASF) was followed by addition of increasing concentrations (ranging from 1 to 25 μM) of galectin (monomer and dimer) to 20 μM ASF (Sigma, St. Louis, MO). Four millimolar β-mercaptoethanol was added as a reducing agent to samples with galectin-1 C3S/V6D. All measurements were performed at 20 or 25 °C.

Fluorescent Probes. Two different probes were used for the fluorescence anisotropy assay, fucosyllactose (**FucLac-probe**) tagged with fluorescein via an ethylamine linker, previously described (*33*), analogous to that used for other saccharides (*34*) and 3′-[4-(fluorescein-5-amidomethyl)-1*H*-1,2,3-triazol-1-yl]-3′-deoxy-β-D-galactopyranosyl 3-(3,5-dimethoxybenzamido)-3-deoxy-1-thio-β-D-galactopyranoside (**tdga-probe** for thiodigalactoside amide) (described in Supporting Information).

Compounds Used for Inhibition Assay. Two previously reported ligands for dRatGal-1w (monovalent **1** and divalent **2**) (*27*), a methyl glycoside of lactose (MeLac), a methyl glycoside of *N*-acetyllactosamine (MeLacNAc), and a biantennary non-asaccharide (N-glycan) were used as ligands (Figure 3). The N-glycan was prepared from a 50:50 mixture of a sialylated and a nonsialylated biantennary oligosaccharide (Isosep AB, Tullinge, Sweden); the oligosaccharides (4.8 mg/mL in water) were desialylated by incubation with 0.1 unit of neuraminidase (sialidase) from *Vibrio cholerae* (Roche, Bromma, Sweden) for 1 h at 37 °C. Free sialic acid was removed by anion-exchange chromatography on a 5 mL HiTrap DEAE FF column (GE Healthcare), at a flow rate of 2 mL of dH_2O/min, and the desialylated glycan was recovered in the flow-through. Successful desialylation and separation were confirmed by NMR.

Fluorescence Anisotropy. The affinities of probes and inhibitors for the different galectins were measured by fluorescence anisotropy and calculated (*34*). A Polar Star plate reader with software FLUOstar Galaxy version 4.11-0 (BMG, Offenburg, Germany) was used. For inhibitors, a fixed concentration of galectin was added to a well of a 96-well microtiter plate (black polystyrene; Costar, Corning, NY) together with a fixed concentration (0.28 μM) of fluorescent saccharide (see above) and one of a dilution series of inhibitor (concentrations ranging from 0.008 to 1 mM). The final concentration of galectin (1 μM dRatGal-1w, 2 μM mRatGal-1, 0.8 μM dHumGal-1w, and 1 μM mHumGal-1) was chosen to give an anisotropy value of about 70 mA without inhibitor. All dilutions were prepared in PBS, and the final sample volume in each well was 200 μL. The plate was incubated under slow rotary shaking in the dark for 5 min before analysis. Fluorescence anisotropy was measured with excitation at 485 nm and emission at 520 nm. Anisotropy was determined without galectin (A_0 representing the free probe), at the experimental condition (A), and at saturating amounts of galectin (A_{max} representing the probe−galectin complex). Fraction of

[1]Abbreviations: FA assay, fluorescence anisotropy assay; dHumGal-1w, dimeric human galectin-1 wild type; dHumGal-1, dimeric human galectin-1 C3S; mHumGal-1, monomeric human galectin-1 C3S/V6D; dRatGal-1w, dimeric rat galectin-1; mRatGal-1, monomeric rat galectin-1 C3S/V6D; FucLac, fucosyllactose; tdga, thiodigalactoside amide; MeLac, Galβ1−4Glcβ-O-Me; MeLacNAc, Galβ1−4GlcNAcβ-O-Me; ASF, asialofetuin.

bound probe was calculated as $(A - A_0)/(A_{max} - A_0)$ and from this fraction bound and free galectin as described (*34*). In the presence of inhibitor, the calculations also included reference values without inhibitor, and also free and bound galectin was calculated as described (*34*). These values could be used to construct binding curves, Scatchard plots, and Hill plots as described in Supporting Information.

Stoichiometry of Galectin−Ligand Interaction. The stoichiometry of the galectin−ligand interaction was evaluated by measuring the fluorescence anisotropy of increasing concentrations of **tdga-probe** (ranging from 0.28 to 11 μM) added to fixed concentrations of galectin (2.5 and 1.25 μM). Scatchard plots were generated by plotting Y = [bound probe/free probe], where free probe was calculated as [total probe] − [bound probe], against X = [bound probe] calculated from anisotropy values as $[(A - A_0)/(A_{max} - A_0)]$[total probe]. Hill plots were generated by plotting $\log(Y/(1 - Y))$, where Y = [fraction of bound CRD] ([bound galectin] = [bound probe]), against $\log(X)$ with X = [free probe].

X-ray Structure Determination of Rat Galectin-1 and Molecular Modeling. The X-ray crystal structure of rat galectin-1 was determined as described in Supporting Information (PDB submission 3m2m). A model of divalent **2** bound to rat galectin-1 was constructed from one of the lactose-bound CRDs (E) of the X-ray crystal structure, using the MMFFs force field in water implemented in MacroModel (MacroModel; 9.1 ed.; Schrödinger, LLC, New York, NY, 2005). A Monte Carlo multiple minima (MCMM) conformational search was performed starting with one of the lactose residues of **2** replacing the lactose in subsite C−D of the carbohydrate binding groove. Only **2** was allowed to relax without restrictions while the protein residues within 8 Å from the binding epitope were constrained with a force constant of 200 kJ/(mol·Å^2). Atoms within 7 Å of the constrained part were frozen. Other atoms were not included in this calculation.

Binding to Fetuin, ASF, LacNAc, and Serum Glycoproteins. Serum sample preparation and affinity chromatography on a galectin-1 column was performed as previously described (*35*). For neuraminidase treatment, 250 μL of serum was mixed with 220 μL of *V. cholerae* neuraminidase (1 unit/mL; Roche) and incubated for 1 h at 37 °C. To test serum's potency to inhibit galectin-1, a fluorescence anisotropy assay was used in an analogous way as previously described for galectin-3 (*35*, *36*), using **tdga-probe** (2.8 μM final concentration) as fluorescent probe, galectin ranging from 0 to ~200 μM, and human serum as inhibitor (50% final concentration). In detail, 9 μL of a probe stock solution was mixed with 81 μL of galectin solution in a microtiter well (96-well plate). Then 90 μL of serum was added and the plate tapped to cause mixing without foaming, and finally anisotropy values were read in a plate reader as described above. The whole procedure was done at room temperature unless stated otherwise, and the time from adding serum until actual reading was 5−10 min. The same assay was also done in the presence of fetuin (Sigma), asialofetuin (ASF) (Sigma) or MeLacNAc instead of serum, and 0.28 μM **tdga-probe**. The percent bound probe was calculated from the fluorescence anisotropy values, and under different assumptions of serum ligand concentration, the percent bound probe with and without serum was used to calculate ligand affinity, fraction of bound ligand, and concentration of free galectin, using the same set of equations in the same way as described previously for inhibitors (*34*). The concentrations of free galectin and bound galectin (= bound ligand) were used to generate Scatchard plots. The fraction of bound ligand was entered as Y and the concentration of free galectin CRD as X to generate Hill plots as described above.

Modeling of Binding Reactions. All modeling was based on exact solution to simple equations of mass action, without deleting any terms for approximation. All modeling was done using Microsoft Excel. The concentration of dimer for different total galectin CRD concentrations $[CRD]_{tot}$ and monomer−dimer K_ds was calculated by solving for [dimer] in the equation:

$$K_d = [\text{monomer}][\text{monomer}]/[\text{dimer}] \quad (1)$$

$$[\text{dimer}] = T_D/2 - \text{sqrt}(T_D T_D/4 - [CRD]_{tot}[CRD]_{tot}/4) \quad (2)$$

where $T_D = [CRD]_{tot} + K_d/4$ and from this percentage of CRDs in the dimer.

The percent probe bound to galectin was calculated for different combinations of galectin concentrations $[Ga]_{tot}$ (constant or a range), known or assumed inhibitor concentration ($[In]_{tot}$) (range or constant) and affinity (K_{dIn} in μM), and probe concentration $[Pr]_{tot}$. The affinity of galectin for the probe (K_{dPr}) was calculated from the binding curve in the absence of inhibitor as described (*34*). The competition of inhibitor and probe for the galectin binding site represents a general case when two molecules (A and B) compete for the same site (C), where, for example, A is inhibitor, B is probe, and C is galectin CRD. The concentration of each interacting partner at equilibrium is governed by two competing equations of mass action and was modeled as follows:

$$K_{dA} = [A][C]/[AC] \quad (3)$$

$$K_{dB} = [B][C]/[BC] \quad (4)$$

[AC] was then calculated from eq 3) using

$$[AC] = T_A/2 - \text{sqrt}(T_A T_A/4 - [C]_{tot}[A]_{tot}) \quad (5)$$

where $T_A = [C]_{tot} + [A]_{tot} + K_{dA}$. Then $[C]_{tot}$ was reset to represent all galectin not bound by A:

$$\text{new } [C]_{tot} = \text{old } [C]_{tot} - [AC] \quad (6)$$

[BC]was then estimated from eq 4 but using the new $[C]_{tot}$

$$[BC] = T_B/2 - \text{sqrt}(T_B T_B/4 - [C]_{tot}[B]_{tot}) \quad (7)$$

where $T_B = [C]_{tot} + [B]_{tot} + K_{dB}$. Then $[C]_{tot}$ was reset to represent all galectin not bound by B:

$$\text{new } [C]_{tot} = \text{old } [C]_{tot} - [BC] \quad (8)$$

The sequence 5−8 was repeated nine times to generate an approximation of bound probe in the presence of inhibitor. Convergence of the algorithm was confirmed by comparing the last two calculations of [BC], which differed by < 1%.

The same type of iterative modeling was used for other situations where two binding reactions compete. For example, when MeLac binds dimeric galectin-1, binding the first CRD is represented by A, the second by B, and MeLac by C. The cooperativity is included in the model by letting the concentration of bound CRD1 (AC) determine the total available CRD2 (i.e., $[B]_{tot}$) in eqs 4 and 7. The total concentration of CRD1 for eq 3

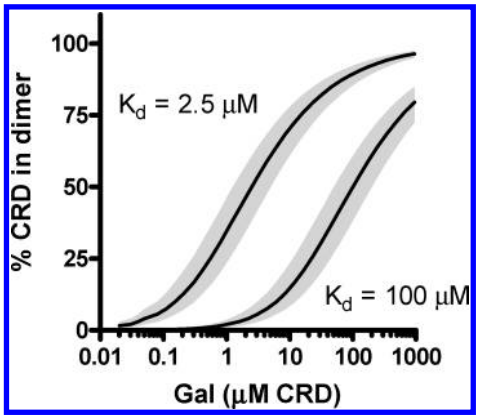

FIGURE 2: Dimerization of galectins. The variation of percent dimer with total galectin concentration under different assumption of K_d of the monomer−dimer equilibrium was calculated, without approximation, from the mass action formula K_d = [monomer][monomer]/[dimer]. The best estimate (lines) with 2-fold variation in either direction (shaded area) is shown for dHumGal-1 (left) and mHumGal-1 (right).

(i.e., $[A]_{tot}$) was either set to half of the total CRD concentration (treating the whole dimer as one reaction partner similar to the model in ref *37*). Alternatively, the total concentration of CRD1 is the same as the total CRD concentration, but for each CRD1 bound two are made unavailable in eq 3), giving the following modification of calculation 5:

$$[AC] = T_A/2 - \mathrm{sqrt}(T_A T_A/4 - [C]_{tot}[A]_{tot}/2) \qquad (9)$$

where $T_A = [C]_{tot}/2 + [A]_{tot} + K_{dA}/2$. Either model gave similar results.

To model binding to dimer in the presence of monomer, the monomer concentration was added as a constant factor to the concentration of CRD2 in the calculations above. This assumes the approximation that the affinity of CRD2 is the same as for the monomer, which is close but not exact.

Linear and nonlinear regression and plotting and layout of figures containing binding data and models were done with Prism 4 (GraphPad Software Inc., San Diego, CA).

RESULTS

Characterization of Galectin-1 Proteins. To address the role of ligand interactions with a single CRD of galectin-1 vs interaction involving cross-linking by two CRDs, we used wild-type and mutant proteins with normal ability to dimerize (dHumGal-1w, dHumGal-1, dRatGal-1w) and other mutants with strongly reduced ability to dimerize (mHumGal-1, mRatGal-1). These have been characterized by others (*38*, *39*) and in addition here as described in detail in Supporting Information (Figures S1−S5). Important for interpretation of both the new and published data are the facts that monomers and dimers are in rapid equilibrium (minutes at room temperature), and theoretical "dimerization curves" (Figure 2) show that, at equilibrium, both monomers and dimers are expected to occur over a wide range of concentrations. In this figure we have estimated the monomer−dimer equilibrium K_d for dHumGal-1 and mHumGal-1, based on size exclusion chromatography (Stowell et al. (*39*) and Supporting Information Figure S1), fluorescence anisotropy (Supporting Information Figure S2), and dynamic light scattering (Supporting Information Figure S3), and shown it to be consistent with the galectins' sensitivity to oxidation (Supporting Information Figure S4) and ability to cross-link asialofetuin

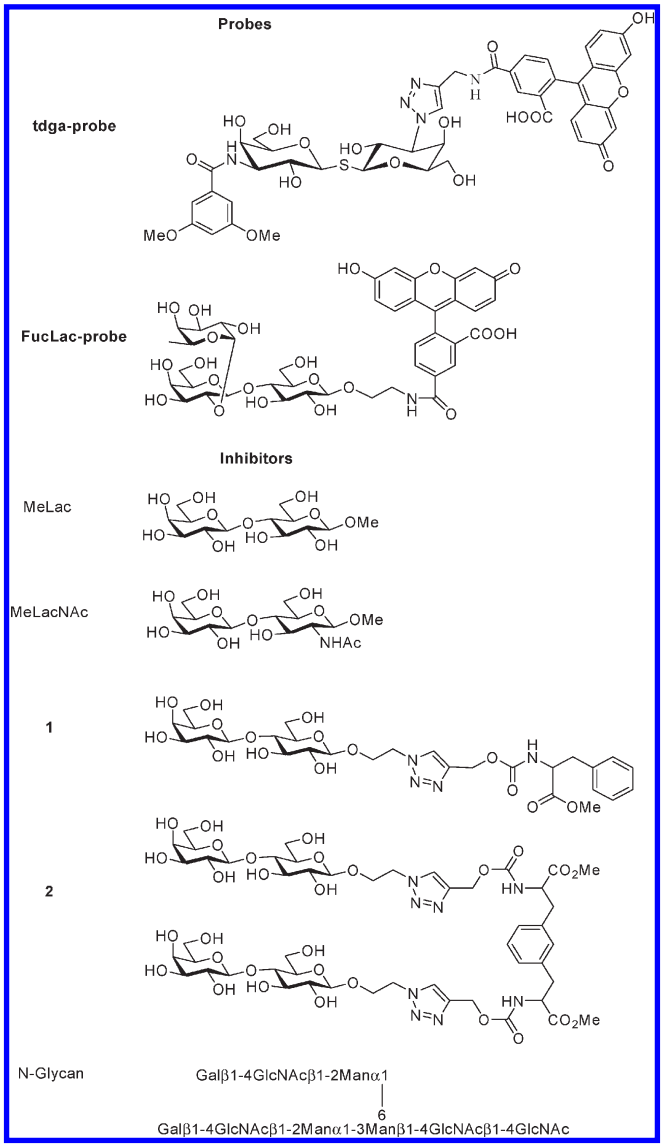

FIGURE 3: Structures of the small molecule galectin-1 ligands tested. The probes **tdga-probe** and **FucLac-probe** used for fluorescence anisotropy and the inhibitors (MeLac, MeLacNAc, monovalent **1**, divalent **2**, and biantennary N-glycan) are shown. A description of the **tdga-probe** synthesis is shown in Supporting Information Scheme S1.

(Supporting Information Figure S5) and cells (Figure S1 and publications by others exemplified in Supporting Information).

Galectin-1 interaction with two fluorescent probes was used for the FA assay: the previously described fucosyllactose based (**FucLac-probe**) compound at high galectin concentration (> ~10 μM) and a newly designed, much more potent thiodigalactoside amide (**tdga-probe**) based probe at low galectin concentrations (< ~10 μM) (Figure 3). The **tdga-probe** is a fluorescinated derivative of a member of a new class of small potent galectin inhibitors, which bind the canonical lactose binding site (C−D in Figure 1) where the thiodigalactose moiety sterically mimics lactose as shown by their competitive inhibition and molecular modeling (*40*), and by X-ray crystallography of thiodigalactose itself in complex with human galectin-1 (*41*). The interaction of the probes with the different galectin-1 proteins was analyzed by measuring fluorescence anisotropy of a low concentration of probe (0.1−0.3 μM) in the presence of increasing concentrations of galectin (~0.1−500 μM) (Supporting Information Figures S2, S6A,B, and S7A,B) as described (*34*).

From the position and shape of the binding curve, the K_d of the binding of **tdga-probe** to monomeric and dimeric dHumGal-1 was estimated to ~0.4 μM and for mHumGal-1 to ~0.7 μM as described in Supporting Information (Figure S2). Since galectin is in large excess over the probe in most of this analysis, the data represent binding to the first CRD of dimeric galectin. For more detailed assessment of stoichiometry and affinities, a range of concentrations of **tdga-probe** was analyzed with two fixed concentrations of galectin, 1250 and 2500 nM, respectively (Supporting Information Figure S6C−F). Scatchard analysis showed that 2477−2542 nM probe bound to 2500 nM galectin CRD and 1119−1220 nM to 1250 nM galectin CRD, demonstrating a 1:1 ratio of CRD to **tdga-probe**, both for dHumGal-1 and for mHumGal-1. At these concentrations dHumGal-1 occurs as a mixture of similar concentrations of monomer and dimer, and mHumGal-1 occurs mainly as monomer with only a few percent dimer. The close to straight lines showed that monomer and either CRD of the dimer of dHumGal-1 bound with close to equal affinity, as construction of model Scatchard plots showed that a difference by a factor of more than 3 would give a clearly visible curvature (not shown). This was confirmed by Hill plots constructed from the same data, which were straight lines of slope close to 1. The affinities of the interactions, derived from the Scatchard plots (K_d = −1/slope) and Hill plots (K_d = *X*-intercept/slope), were about 0.6 μM for dHumGal-1, representing an average of the molecular species present, and about 0.9 μM for mHumGal-1 (Supporting Information Figure S6), and similar for the rat galectin-1s (not shown). These values are in good agreement with those obtained from Supporting Information Figure S2, although slightly higher, which may be due to experimental variation and also the fact that the second CRD of dimeric galectin-1 is included in the estimates from Supporting Information Figure S6C−F. The **FucLac-probe** bound both human galectin-1s with about equal K_d ~110 μM (Supporting Information Figure S7A,B), possibly reflecting the fact that mHumGal-1 also is mainly a dimer at the higher concentrations assessed by this probe. The binding curve shape (Supporting Information Figure S7A) and the Hill plot (Supporting Information Figure S7B) were both consistent with a 1:1 stoichiometry between **FucLac-probe** and each galectin-1 CRD; a Scatchard plot could not be constructed as it would consume too much probe to make it reliable at this relatively low affinity.

Galectin-1 interaction with MeLac and MeLacNAc was evaluated to compare the two probes in the competitive fluorescence anisotropy assay (*27*, *34*, *42*) and also to look for evidence for the recently reported negative cooperativity of binding of lactose to galectin-1 (*37*). In the first type of assay, a fixed concentration of fluorescent probe (0.1−0.3 μM) and galectin was analyzed with different concentrations of inhibitor (Table 1) as described before. By comparison with the interaction without inhibitor, the fluorescence anisotropy, which is directly related to the fraction of bound probe, can be used to estimate the concentration of free galectin (for each inhibitor concentration), which in turn permits calculation of inhibitor bound galectin (total − free − probe-bound), and from these K_d values. This estimate of free galectin works even if the galectin consists of both dimer and monomer, since the affinities of each for the probe are close to equal, as described above. For most informative data points, we selected a galectin concentration giving 40−90% binding in the absence of inhibitor and ~20−80% inhibition with inhibitor; the more outside this range the more sensitive to measurement errors the calculation will be. For the high-affinity **tdga-probe** the optimal galectin concentration was ~1 μM, and for the lower affinity **FucLac-probe** it was ~200 μM at room temperature. Thus, assay with the two probes measures interactions with two very different concentrations of galectin, with the possibility of observing different effects due to this, but also limiting the use of the **FucLac-probe** to inhibitors available in large enough amounts to inhibit the higher concentration of galectin.

Table 1: Affinity (K_d in μM) of Ligands for Dimeric and Monomeric Rat and Human Galectin-1[a]

galectin	μM	Inh	Val	K_d
dRatGal-1w	1	MeLac	1	310
dRatGal-1w	1	MeLacNAc	1	200
dRatGal-1w	1	**1**	1	210
dRatGal-1w	1	**2**	2	25
dRatGal-1w	1	N-glycan	2	130
mRatGal-1	2	MeLac	1	540
mRatGal-1	2	MeLacNAc	1	300
mRatGal-1	2	**1**	1	240
mRatGal-1	2	**2**	2	35
mRatGal-1	2	N-glycan	2	100
dHumGal-1w	0.8	MeLac	1	300
dHumGal-1w	0.8	MeLacNAc	1	210
dHumGal-1w	0.8	**1**	1	130
dHumGal-1w	0.8	**2**	2	8.9
dHumGal-1w	0.8	N-glycan	2	110
mHumGal-1	1	MeLac	1	380
mHumGal-1	1	MeLacNAc	1	230
mHumGal-1	1	**1**	1	170
mHumGal-1	1	**2**	2	16
mHumGal-1	1	N-glycan	2	190

[a]Averages of the K_ds calculated from fluorescence anisotropy data with fixed concentrations of probe (0.28 μM **tdga-probe**) and galectin and a range of different concentrations of inhibitors (~10 to ~500 μM) as described by Sorme et al. (*34*).

To compare the two probes in detail in an inhibition assay, we analyzed a range of MeLac concentrations with the two galectin-1s, each tested at two concentrations (~1 and 200 μM) corresponding to the probe used (Supporting Information Figure S8). The results looked very similar for all four combinations, when presented as percent inhibition of anisotropy (Supporting Information Figure S8A) or recalculated as percent MeLac bound galectin (Supporting Information Figure S8B), except that dHumGal-1 at the higher concentration showed a slight difference. A more detailed analysis of this revealed a clear difference suggesting negative cooperativity of the binding of MeLac to dHumGal-1. In a Scatchard plot (Supporting Information Figure S8C), the data fit a model curve shape for a K_d of 65 μM for binding of MeLac to the first CRD and K_d ~650 μM for binding to the second CRD and a Hill plot (Supporting Information Figure S8D) with slope 0.76, all in good agreement with the previous report (*37*). dHumGal-1 at the lower concentration (0.8 μM), however, did not show negative cooperativity with the same concentration range of MeLac (Supporting Information Figure S8E). A reasonable explanation for this would be that 0.8 μM contains much less dimer. To examine this, we compared the data for different dHumGal-1 concentrations with model curves for different percentages of dimer (taken from Figure 2) in a normalized Scatchard plot (Supporting Information Figure S8F). A decrease of dimer will expand the low slope part of the curve due to increased contribution of monomer. Thereby, the steep part of the curve will be pushed to the left, and for 0.8 μM dHumGal-1 it will fall outside the range

of tested MeLac concentrations. An intermediate dHumGal-1 concentration (12 μM) gave the expected degree of intermediate evidence for cooperativity. mHumGal-1 showed little signs of cooperativity even at the high concentration (Supporting Information Figure S8C), which cannot be explained only by its lower percentage of dimer (~60%) but also by other factors, perhaps a different quality of the dimer interface.

An alternative analysis with a fixed inhibitor concentration and a range of galectin concentrations as exemplified for the MeLacNAc−galectin interaction gave about the same calculated average affinity (K_d ~200 μM) when tested at either low (with **tdga-probe**, in Supporting Information Figure S6A,B) or high (with **FucLac-probe**, Supporting Information Figure S7A) galectin concentration range. Modeling of the curve slopes and shape is consistent with a single site 1:1 interaction (Supporting Information Figure S7A), but there is a slight difference between the two galectins in the derived Hill plots of log(free galectin CRD) vs log(bound MeLacNAc/free MeLacNAc) (Supporting Information Figure S7C). mHumGal-1 shows a slope of close to 1, but dHumGal-1 has a slope of ~1.25 indicating negative cooperativity of the binding of MeLacNAc to the dimeric galectin, as recently suggested for lactose (*37*) and described above for MeLac.

Analysis of the Galectin-1 Interaction with Small Divalent Molecules. Next we analyzed a synthetic bivalent lactose derivative, compound **2** in figure 3, and a natural bivalent ligand, a biantennary N-glycan. With fixed low concentrations (~1 μM) of either dHumGal-1 (containing ~30% dimer) or mHumGal-1 (containing ~2% dimer), the measured affinity of **2** was 10−15 μM, which is 10−15 times higher than found for its monovalent counterpart **1** (Table 1). Results consistent with this were also obtained when a range of galectin concentrations were tested with a fixed concentration (20 μM) of **1** or **2** (Supporting Information Figure S9). This increased affinity of **2** over **1** is higher than can be explained by the double number of lactose moieties in **2**. It can also not be accounted for by dimerization of the galectin, since it was seen to an equal or even stronger degree with the dimerization deficient mHumGal-1. The cross-linking of two galectin-CRDs by one molecule of **2** is also not likely, since the inhibition data points agree with a 1:1 CRD **2** interaction but not with a 2:1 interaction (Figure 4A), and dynamic light scattering did not show any sign of cross-linking of dHumGal-1 by **2** (Figure 4B). Thus, it is most likely that particular structural features of **2** are more important for its affinity for galectin-1 than its valency *per se*. In agreement with this, the biantennary N-glycan had no enhanced affinity compared to MeLacNAc and bound with equal affinity to both dimeric and monomeric galectin-1. A series of mono-tetravalent lactosides also had affinities only in proportion to their content of lactose, with no further enhancement due to multivalency (*43*).

Modeling of the Interaction between Monomeric Galectin-1 and a Divalent Ligand. To identify a possible structural basis for the enhanced interaction between compound **2** and a galectin-1 CRD, a model was built, based on a lactose-bound CRD from the X-ray crystal structure of rat galectin-1 described in Supporting Information (PDB 3m2m), a canonical galectin β-sandwich structure essentially identical to the solved structures of human (*44*) and bovine (*45*) galectin-1, except for the ~15% aa side chains that are different between the species. In Figure 5 the surface of one rat galectin-1 CRD is shown in three projections, with differences to human galectin-1 highlighted by yellow or red color. The ligand is shown as stick models in two low-energy

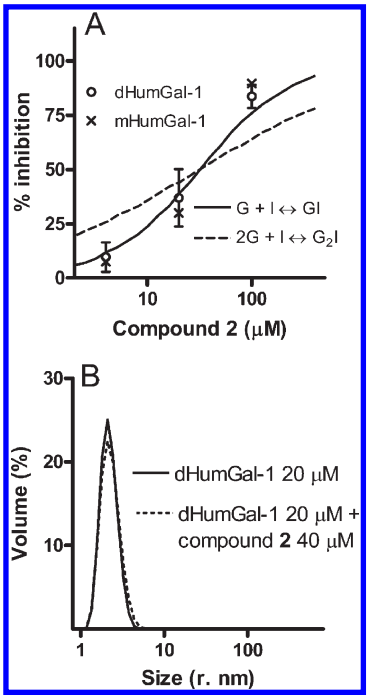

FIGURE 4: Interaction of galectin-1s with compound **2**. (A) The inhibition of interaction between galectin-1s and **tdga-probe** by different concentrations of **2** (*X*-axis) was measured by fluorescence anisotropy. Theoretical curves were calculated for two stoichiometries of the galectin−inhibitor interaction (same IC_{50}). The data are consistent with the 1:1 interaction but not with the 2:1 interaction. The data are from six independent experiments, with duplicate samples in each for each data point. The 95% confidence intervals are shown by bars for dHumGal-1 and were of the same magnitude for mHumGal-1 (not shown). (B) Dynamic light scattering of 20 μM dHumGal-1 in the absence and presence of 40 μM **2**.There was no sign of cross-linking as the peaks closely overlap.

conformations found by molecular dynamics simulation. This revealed that while one lactose moiety (Lac1 in Figure 5) is bound in the canonical core site (Figure 5A), the remainder of the ligand is quite mobile, and part of the time the arm with the other lactose moiety (Lac2) projects out into solution (light blue in Figure 5). However, part of the time Lac2 wraps around the protein surface (green in Figure 5) and puts its lactose moiety near residues on the other side of the galectin CRD (Figure 5C), suggesting the possibility of interactions there. Even though these interactions are expected to be weak and transient, they may explain affinity enhancements of **2** over **1** (Table 1) as explained in the Discussion.

Analysis of the Galectin-1 Interaction with Glycoproteins: Asialofetuin and Fetuin. To explore the possibility of using the fluorescence anisotropy assays described above for analysis of galectin-1 interaction with glycoproteins in solution, we first analyzed asialofetuin, a commonly used model glycoprotein known to bind galectin-1. Fetuin has three N-glycans and three O-glycans. The N-glycans are mainly triantennary, but also di- and tetrantennary occur (*46*). Most antennae have LacNAc residues mainly capped by 2−3 sialic acid, but also 2−6 sialic acid and uncapped. Removal of the sialic acids produces ASF, with on average nine terminal LacNAc residues in the N-glycans, and about nine galectin-1 binding sites (*47*). At first we used the same assay as for small molecule inhibitors described above (Table 1), with a range of concentrations (3−80 μM) of ASF as inhibitor and fixed concentration of galectin (~1 μM) and the **tdga-probe** (0.28 μM); the ASF concentrations were multiplied with different

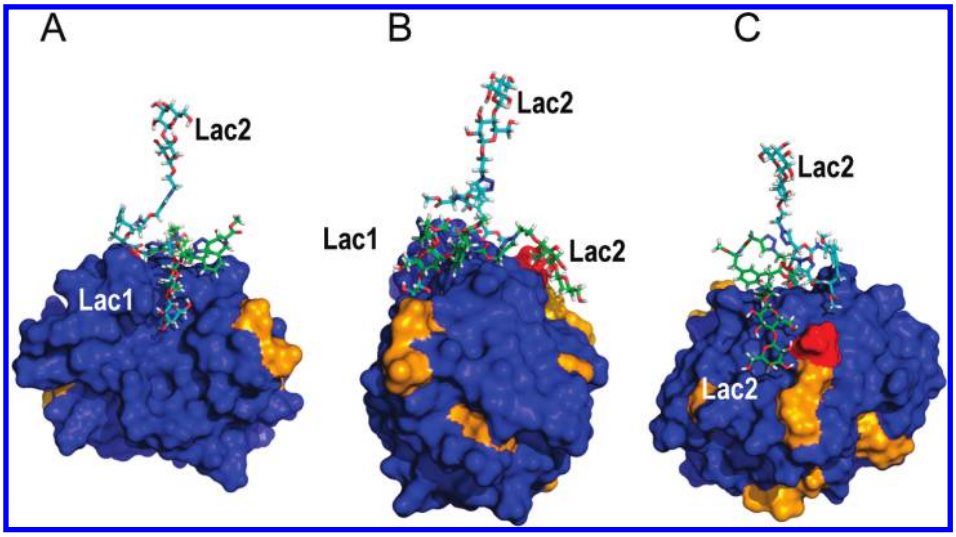

FIGURE 5: Model of interaction of divalent compound **2** with a galectin-1 CRD. The surface of a rat galectin CRD is shown with stick models of two low energy conformations of **2** (green and light blue carbons, respectively; oxygens are in red in both) derived from a conformational search. The conserved parts of the galectins (amino acids identical to human galectin-1) are colored blue, and the different parts are in yellow and red. Three views are shown: (A) the "carbohydrate binding side" (= S-side (*29*)) with lactose1 bound to subsite C and D, (B) side view, and (C) the "back side" (= F-side); Lac2 is either projected out into solution (light blue) or wrapped around the protein near aa75 (shown in red), which is Thr in RatGal-1 and Ala in HumGal-1. The picture was made using PyMOL, DeLano Scientific LLC.

Table 2: Affinities of ASF and Fetuin for Galectin-1 (K_d in μM)[a]

inhibitor	sites	dHumGal-1	mHumGal-1
ASF	1	2.6	15
ASF	9	25	140
fetuin	1	35	77
fetuin	9	320	690

[a]FA assay was done as in Table 1, with 3−80 μM ASF or fetuin as inhibitor and assuming 1 or 9 binding sites per molecule.

trial values, representing numbers of galectin binding sites per molecule, to obtain the inhibitor concentrations used in the calculations of K_d. The inhibitory potency of ASF was consistent with the presence of one galectin binding site per molecule with K_d of ~3 μM for dHumGal-1 and a K_d of ~15 μM for mHumGal-1, or, for example, nine binding sites per ASF molecule with about nine times lower average affinity (Table 2).

To estimate the number of galectin binding sites per ASF molecule, a range of galectin concentrations was analyzed in the presence of a fixed concentration of ASF, 20 μM (Figure 6A) or 40 μM (not shown), and probe. The binding curve shifted less to the right for mHumGal-1 (Figure 6A inset), indicating less inhibition by ASF than for dHumGal-1 consistent with the inhibition data of Table 2. The fluorescence anisotropy values were used to calculate the concentrations of free galectin and in turn the concentrations of ASF-bound galectin (total galectin − free galectin − probe-bound galectin) as described for small molecules above. With the high-affinity **tdga-probe**, giving most informative data points in the low galectin concentration range (~1−10 μM), Scatchard analysis (Figure 6B) indicated slightly less than 1 site per ASF molecule (13 μM sites on 20 μM ASF) with a K_d of ~3 μM for dHumGal-1, and similar for mHumGal-1 (17 μM sites on 20 μM ASF), but with lower affinity (K_d of ~10 μM). The lower affinity binding sites on ASF are not well detected in this analysis because when galectin concentration is high enough to show significant binding to them, it is also high enough to saturate the **tdga-probe**.

Therefore, we used the lower affinity **FucLac-probe**, giving the most informative data points in a higher galectin concentration range (~50−300 μM), to investigate lower affinity galectin-1 binding sites on ASF. In this concentration range, both galectins bound about equally to ASF, as illustrated by almost identical plots of percent bound probe vs added galectin concentration (Figure 6C). The average affinity of the galectins for 20 μM ASF was about equal to 0.4 mM MeLacNAc as half-maximum of the binding curves were similar, but the clearly steeper binding curve with ASF, upward concave Scatchard plots (not shown) and Hill plots with negative slopes (not shown), indicate negative cooperativity of galectin-1 binding to ASF as has been proposed (*47*) and/or a range of different affinities (K_d ~10−600 μM) for the different binding sites. When the calculated ASF-bound galectin was plotted against added galectin (Figure 6D), the data could not, as expected, be fit to a single affinity binding site, and instead a two binding site model is shown (as described in legend to Figure 6D). With this, the data were consistent with the presence of about nine galectin-1 binding sites per ASF molecule, since the curves approached a total of about 360 μM for 40 μM ASF and 180 μM for 20 μM ASF in agreement with published data (*47*).

A potential complicating factor in the high galectin concentration range is the rapid formation of large ASF−galectin precipitates, which were clearly visible in the present experiments and detected by dynamic light scattering (Supporting Information Figure S5). To asses their influence on the results, we prepared larger volume samples of the same composition, centrifuged half at 20000*g* for 5 min, and compared the now cleared supernatant to the unseparated sample. There was no significant difference in the total measured fluorescence (< 2%) (Supporting Information Table S2) or anisotropy (Supporting Information Figure S10), and analysis of a sample without added fluorescent probe showed that light scattering of the precipitates themselves contributed < 0.5% to the signal in the emission channels (see legend to Supporting Information Figure S10). These data show that optical effects of the precipitates do not significantly perturb the anisotropy measurements. Since the

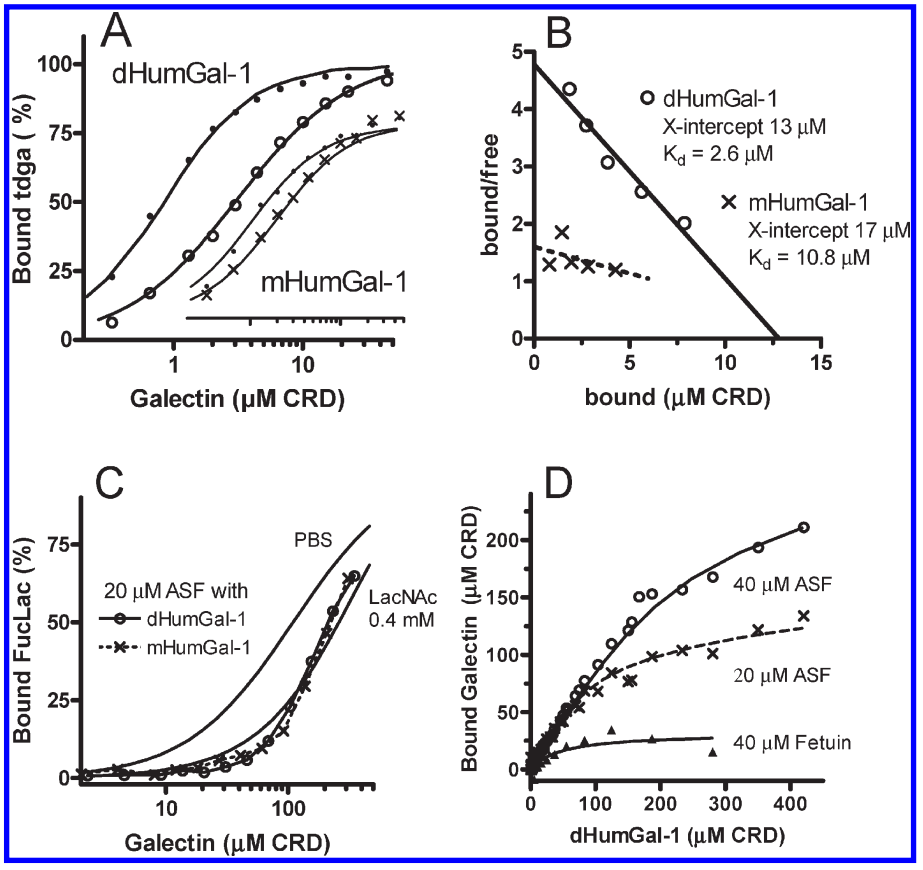

FIGURE 6: Interaction of galectin-1 with asialofetuin (ASF) and fetuin. (A) A range of concentrations (*X*-axis) of dHumGal-1 or mHumGal-1 (inset) were mixed with 0.28 μM **tdga-probe** as probe and either 20 μM ASF (right curves) or PBS (left curves), analyzed for fluorescence anisotropy, and % bound probe calculated (*Y*-axis). Data points are shown as filled dots (PBS) or symbols as explained in panel B (ASF), and fitted theoretical binding curves are shown as unbroken lines. (B) Scatchard plots were generated using the concentrations of free and bound galectin calculated from the data of panel A. (C) A plot analogous to panel A but with 0.1 μM **FucLac-probe** as probe and besides 20 μM ASF including 0.4 mM MeLacNAc as inhibitor for comparison. For ASF the data points are shown with connecting lines for each galectin as indicated. For PBS and MeLacNAc only the best fitting theoretical binding curves are shown for clarity, in each case with a high goodness of fit ($R^2 = 0.99$). (D) Plots of ASF-bound dHumGal-1 concentrations were calculated from the data of panel C and additional similar experiments (total of 33−47 data points for each ASF curve), with fitted curves assuming 9 galectin binding sites per ASF molecule, half with K_d 20 μM and half with K_d = 600 μM. In addition, a plot of dHumGal-1 binding to fetuin is shown, with a fitted curve corresponding to 30 μM binding sites with K_d = 50 μM. Plotting and layout were made using Prism 4, GraphPad Software Inc.

precipitates contained no or little of the fluorescent probe (Supporting Information Table S2), the percent bound probe (Figure 6 and Supporting Information Figure S10) reflects the concentration of free galectin CRD in solution. For example, with 20 μM ASF and 90 μM total galectin CRD (as in Supporting Information Table S2), 20 μM galectin CRD was free. Since this accounts for about half of the soluble material (~0.3 mg = 15% in Supporting Information Table S2), about 80% of the bound galectin (70 μM) and ASF must be in the precipitates. This would give a galectin CRD/ASF ratio of 3−4 to 1, which is in agreement with published data (*48*−*50*). Thus, the precipitates may account for a large part of the bound galectin calculated as in Figure 6D. Further studies of this are beyond the scope of the present paper, except the following observations.

ASF−galectin precipitates did not form in low salt buffer (10% PBS, Supporting Information Table S2). Therefore, we compared the affinity of ASF for dHumGal-1 in 10% PBS and PBS (Supporting Information Table S3). While the high-affinity site, detected with **tdga-probe**, had changed only a little, the average affinity of the other sites on ASF was reduced by a factor of 4−5.

Intact fetuin was analyzed because most of its LacNAc residues are capped by 2−3 sialic acid (*46*), which, in contrast to 2−6 sialic acid, is well tolerated by galectin-1 (*51*), and we wanted to compare its binding to dHumGal-1 with the N34D mutant galectin-1 that has lost this tolerance (described below). However, fetuin was a very poor ligand for both dimeric and monomeric galectin-1 (Table 2), and the analysis of Figure 6D suggested about one galectin binding site per molecule with K_d ~40 μM. Further confirmation of this surprising result was that <1% of fetuin bound to a galectin-1 column, whereas almost all ASF bound (not shown); a K_d of <5 μM is required for binding to this column as shown by control experiments and modeling (*35*).

Interaction of Galectin-1 with Serum Glycoproteins. Human serum provides a well-characterized array of easily accessible, biologically relevant galectin ligands (*35*); a selected set of human serum glycoproteins binds galectin-1 by affinity chromatography.[2] Therefore, we analyzed the presence of high-affinity galectin-1 binding sites on serum glycoproteins, and the role of galectin-1 dimerization, in an analogous way as described for ASF above; a dilution series of galectin-1 was mixed with a fixed concentration of **tdga-probe** in the presence and absence of

[2]M. C. Carlsson, C. Cederfur, V. Schaar, A. Lepur, M. Fernö, H. Olsson, and H. Leffler, Large increase of galectin-1-binding serum glycoproteins in breast cancer patients, manuscript in preparation. Part included in a Ph.D. thesis (Cecilia Cederfur, Lund University, 2008).

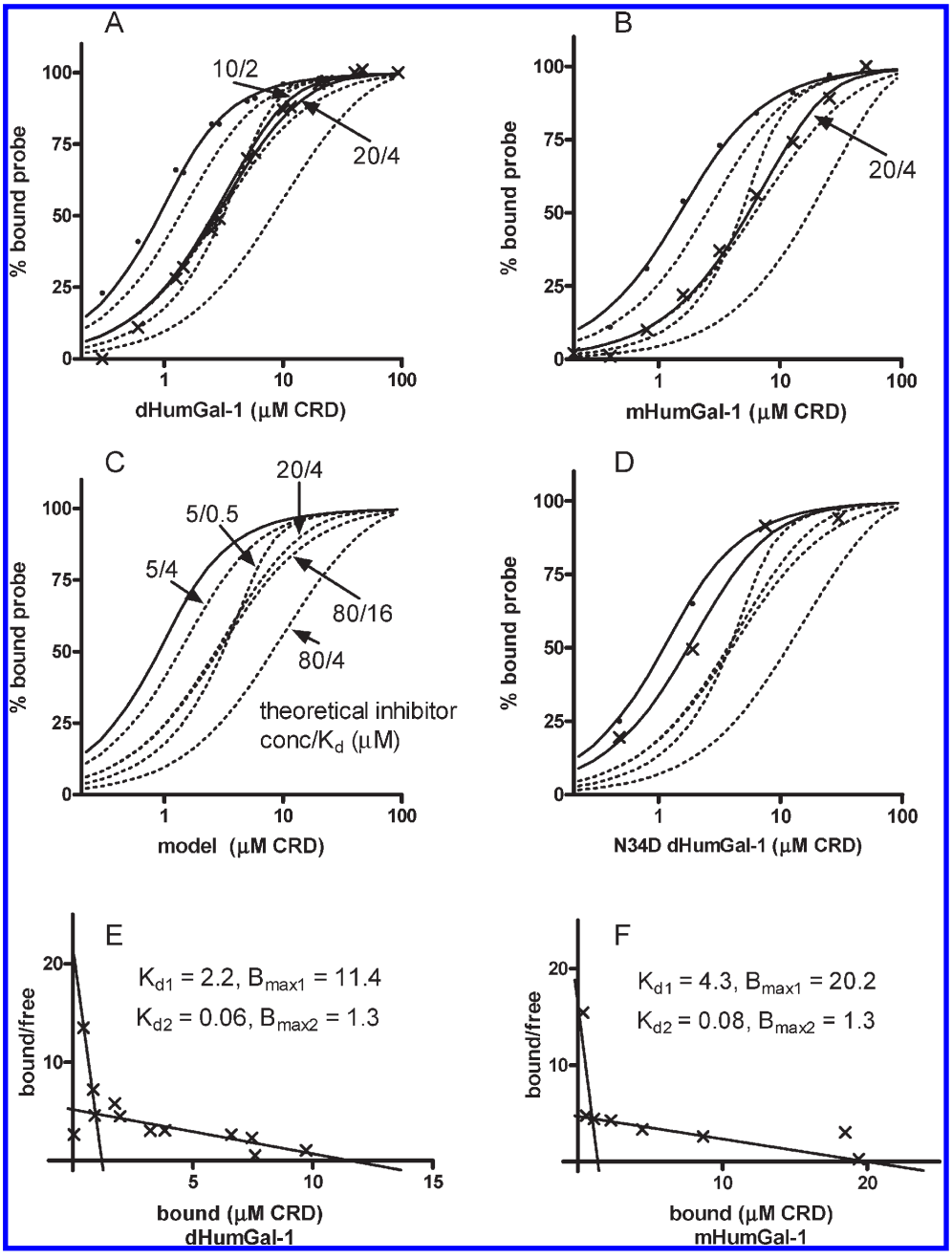

FIGURE 7: Interaction of human galectin-1 with human serum glycoproteins. (A−D) A range of galectin concentrations (given as concentration of CRDs on *X*-axis) were mixed with 2.8 μM **tdga-probe** as probe and either 50% human serum (final concentration) or PBS, analyzed for fluorescence anisotropy, and % bound probe calculated (*Y*-axis). Data points with serum are shown as × and without serum as small filled circles. Theoretical binding curves were calculated for the case without serum (unbroken line furthest to the left) and under different assumption of ligand concentration/K_d in 50% serum as indicated in panel C (dotted lines). For each galectin (panels A, B, and D), the best fitting curves are shown as unbroken lines, and the others as dotted lines. (E, F) Scatchard plots were generated using the concentrations of free and bound galectin calculated from the data of panels A and B, as described under Experimental Procedures. Plotting, linear regression, and layout were made using Prism 4, GraphPad Software Inc.

50% human serum (instead of ASF), and the percentage of **tdga-probe** bound was determined by the measured anisotropy values as described for serum-containing samples (*35*). Reducing agents, as often used with galectin-1, were not included in order not to disturb the structure of the serum glycoproteins. Therefore, we carefully assessed the inactivation of galectin-1 in serum, using the FA assay as described in Supporting Information (Table S4), and found that it could be avoided by the speed of the assay (< 15 min). The C3S mutant (dHumGal-1) was used for most experiments, to increase resistance to oxidation, but all data were also confirmed using wild-type galectin-1.

It was clear that the galectin−tdga interaction was inhibited by serum, since the binding curve shifted to the right (Figure 7) and by about the same magnitude for the dHumGal-1 and mHumGal-1. To further confirm that this curve shift represents competitive inhibition of galectin by serum glycoproteins, we also analyzed the C3S/N34D mutant (= the N34D mutant of dHumGal-1) as a negative control. This mutant, described in more detail below, has lost most binding to serum glycoproteins (75% as assessed by affinity chromatography, Figure 8A) but retains affinity for the **tdga-probe** (Figure 7D). As expected for competitive inhibition by less ligands in serum, its binding curve

had shifted only corresponding to the presence of about 25% as much inhibitory ligand compared to dHumGal-1 (Figure 7D). This validates the assay and confirms that most of the interaction of galectin-1 with serum glycoproteins is mediated by its carbohydrate recognition site.

The concentration of the galectin-1 binding sites (inhibitors) found in serum (mainly LacNAc moieties of serum glycoprotein N-glycans) and their affinity for galectin-1 were estimated in two ways. In one, the concentrations of free and bound (to serum glycoproteins) galectin CRD were calculated from the fluorescence anisotropy data as described in Experimental Procedures and for the experiments with ASF above and analyzed by Scatchard plots (Figure 7E,F). This suggested a major binding site with concentration of 11.4 μM and K_d 2.2 μM for the dHumGal-1 and concentration of 20.2 μM and K_d 4.3 μM for mHumGal-1. In another analysis, to better assess sensitivity of the conclusions to experimental variation, we calculated a series of theoretical binding curves for different trial values of inhibitor concentration and affinity (Figure 7C) and compared them to the experimental curves (Figure 7A,B). The data for both dHumGal-1 and mHumGal-1 were most consistent with a theoretical binding curve based on a 20 μM inhibitor concentration (in the 50% serum tested) with an average K_d of 4 μM. Much lower (e.g., 5 μM) or higher (e.g., 80 μM) estimates of the inhibitor concentration with the same affinity gave clearly different binding curves, as seen in Figure 7C. Curves with a similar position along the *X*-axis could be obtained with different combinations of concentration and affinity, but they either had a lower (e.g., conc/K_d = 80/16) or a higher slope (5/0.5). The concentration and affinity of binding sites suggested by the Scatchard plot for dHumGal-1 (conc/K_d = 10/2) generated a curve that diverged from the data as little as the one for conc/K_d = 20/4 (Figure 7A), but in opposite direction. Therefore, a best estimate of binding site concentration may be 15 μM (in 50% serum) for dHumGal-1. For mHumGal-1, both types of analyses suggested binding sites in 50% human serum at a concentration of 20 μM and affinity of K_d ~4 μM. Although based on few data points, the Scatchard plots (Figure 7E,F) also suggested the possibility of lower concentration (~1.3 μM) of higher affinity (K_d ~0.6−0.8 μM) galectin-1 binding sites, but again equal for the dHumGal-1 and mHumGal-1.

To gain further insight into the stoichiometry and possible cooperativity of galectin-1 interaction with serum glycoprotein binding sites, Hill plots (Supporting Information Figure S11) were generated from the data points for 0.5−20 μM added galectin taken from the same experiments as shown in Figure 7A,B, respectively, and using the concentrations of major binding sites on serum glycoproteins from the Scatchard plots (Figure 7E,F). Both galectins gave linear Hill plots with slopes close to 1 (0.88 and 0.97, respectively). This is consistent with a model where the two CRDs bind ligand with about equal affinity one at a time and where the binding of one does not influence the likelihood that the other would bind very much. The fact that the slope is slightly lower than one for dHumGal-1 may indicate a slight deviation from this model.

From the analysis described above, it can be concluded that the affinity of dimeric and monomeric human galectin-1 for serum glycoproteins is at least about 30 times higher than that for the nonsialylated biantennary N-glycan (Table 1) and about 50 times higher than that for MeLacNAc. Thus, there is a clear affinity enhancement of serum glycoproteins for galectin-1, compared to these component saccharides. This affinity enhancement is not due to dimer-dependent effects (cross-linking of binding sites and cooperativity), as mHumGal-1 bound serum glycoproteins with about equal affinity. It is also not due to cross-linking of the galectin by serum glycoproteins, as this would give Hill plots with slopes approaching 2 (>1) for a 2:1 galectin CRD:ligand stoichiometry, which was not found (Supporting Information Figure S11).

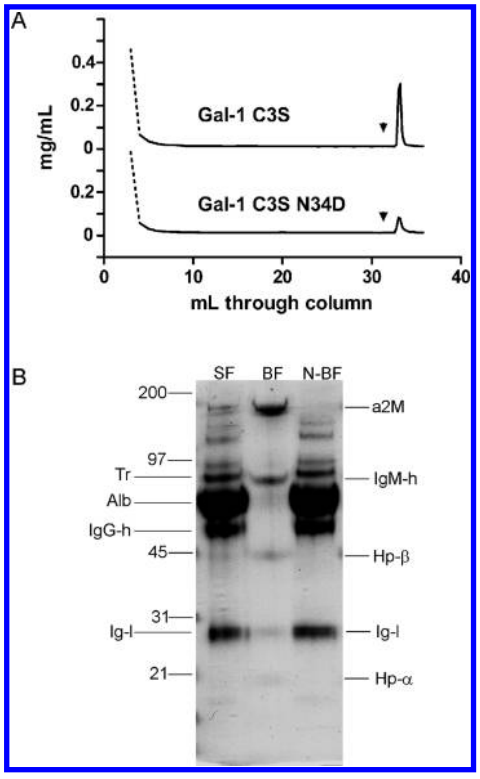

FIGURE 8: Affinity chromatography of human serum on immobilized galectin-1 C3S and C3S/N34D. (A) A 0.1 mL sample of the same serum as used in Figure 7 was diluted to 2 mL in PBS and loaded on a 1 mL column with immobilized galectin-1 C3S (top chromatogram) or mutant C3S/N34D (bottom chromatogram). The column was washed with ~30 mL of PBS, and then elution with 150 mM lactose started (arrowhead). The protein concentration of each collected fraction is given on the *Y*-axis. (B) SDS−PAGE (4−20% stained with Coomassie) of serum (diluted 1/20) before fractionation on immobilized galectin-1 C3S (lane SF), bound and lactose eluted fraction (lane BF), and unbound fraction (lane N-BF). Indicated to the left are the mobilities of known size markers and the main unbound proteins (Tr, transferrin; Alb, albumin, IgG-h, IgG heavy chain, and Ig-l, Ig light chain). Indicated to the right are the mobilities of the main bound proteins seen in middle lane (a2m, α-2-macroglobulin; IgM-h, IgM heavy chain; Hp-*β*, haptoglobin *β*-chain; Ig-l, Ig light chain (from IgM); and Hp-α, haptoglobin α-chain). The indicated proteins were identified by mass spectrometry and for all bound proteins and transferrin also confirmed by Western blot analysis using appropriate specific antibodies as described in ref *35*.

Evidence for a Specific Galectin-1 Binding Site on Human Serum Glycoproteins. Since the affinity enhancement of galectin-1 for serum glycoproteins is not due to the dimeric state or cross-linking, there must be other explanations, such as extended interactions within a single CRD. Evidence for the latter hypothesis is provided by the selective binding of serum glycoproteins to galectin-1 by affinity chromatography (Figure 8), which requires a K_d < 5 μM based on modeling of column behavior (*35*) and, hence, is consistent with the affinity for serum glycoproteins in solution estimated above. Galectin-1 bound ~30% of purified haptoglobin but not transferrin (not shown). This suggests that simply available unblocked (e.g., by

NeuAcα2−6) LacNAc residues are not enough to confer binding but that additional specific features of the bound glycoproteins are required. Further evidence is provided by the fact that < 2% of neuraminidase-treated transferrin bound galectin-1, showing that its predominant asialo-biantennary N-glycan is not enough to confer binding to galectin-1 on the column, requiring an affinity of $K_d < 5\ \mu M$ as described above.

The galectin-1 N34D mutant provides some information on the nature of the specific galectin-1 binding site. This mutant was made among a series of galectin-1 mutants (to be published elsewhere) because residue N34 in site B (Figure 1) is conserved among most mammalian galectin-1s, but the corresponding position in many other galectins is a D (*52*). The fine specificity of galectin-1 C3S/N34D and galectin-1 C3S (=dHumGal-1) was compared in the fluorescence anisotropy assay by direct binding (*34*) to a collection of fluorescein-tagged saccharides (Supporting Information Table S2 in ref *33*) and inhibition by selected soluble saccharides (not shown). Surprisingly, the N34D mutant showed a selective loss of affinity (by a factor of 5−10) for 2−3 sialylated lactose, LacNAc, and Galβ1−3GlcNAc (3, 14, and 17, respectively, in Supporting Information Table S2 in ref *33*), whereas the affinity for the corresponding nonsialylated disaccharides remained essentially unchanged. This suggests that the loss of binding to serum glycoproteins of this mutant (Figure 7D and 8A) is due to lost ability to bind 2−3 sialylated galactose residues, a minor structure type in human serum glycoproteins mainly found on the third antenna of triantennary N-glycans. The apparent preference of wild-type galectin-1 for them may be due either to the fact that the 2−3 sialic acid itself increases binding affinity or to the fact that other aspects of the particular galactoside increases affinity, and the sialic acid must only be tolerated because it is frequently found to cap such a galactoside. To distinguish these possibilities, serum was treated with neuraminidase and analyzed by affinity chromatography on galectin-1 C3S/N34D or galectin-1 C3S (not shown). The second alternative was supported since the neuraminidase treatment restored the ability of serum glycoproteins to bind the C3S/N34D mutant to equal levels as galectin-1 C3S. Had the first alternative been true, one would have expected that neuraminidase-treated serum would decrease binding of galectin-1 C3S instead. These results show that high-affinity binding of galectin-1 to serum glycoproteins is not conferred by any available galactoside but only those in a particular context, as detailed further under Discussion.

As shown in Supporting Information Figure S12 the dimeric and monomeric forms of rat galectin-1 also bind with equal affinity to human serum glycoproteins. However, the data suggested that both bound weaker (by a factor of about 2) relative to human galectin-1, indicating a lower affinity (e.g., same 20 μM ligand concentration with $K_d = 12\ \mu M$) and/or a more restricted set of ligands (e.g., 10 μM ligand concentration with same $K_d = 4\ \mu M$). This may be due to altered interactions outside the main carbohydrate recognition site, where rat and human galectin-1 differ (Figure 5).

DISCUSSION

At the concentrations where galectin-1 is known to induce most of its biological effects (~0.1−10 μM), it exists as a mixture of monomer and dimer, and monovalent binding and dimer-dependent effects (cross-linking (*13*) and negative cooperativity (*37*)) will occur at the same time. Here we show that, in solution at such physiological concentration, dimeric and monomeric forms of galectin-1 bind a variety of ligands with about equal affinity. This includes monovalent and divalent small molecules as well as serum glycoproteins. Even the divalent compound **2** that bound with an apparent cluster effect (enhanced affinity compared to the corresponding monovalent compound) also bound monomeric galectin-1 with enhanced affinity. Serum glycoproteins also bound with enhanced affinity, relative to the component saccharides, both to dimeric and to monomeric galectin-1, again suggesting interactions involving only one CRD. Thus, the enhancement of galectin-1 affinity to the physiological micromolar range does not require the dimerization-dependent effects. These findings raise the questions of what is the mechanism, what are the practical applications, and what are the biological implications.

The present data do not define a precise mechanism for the enhanced binding affinities, which is beyond the scope of the current work, but they provide a basis for discussion of some possibilities and alternatives. The affinity increase of **2** over **1** (10-fold) or certain glycoproteins over LacNAc (30−50-fold) requires only small shifts in binding energy ($\Delta\Delta G$ of 6−10 kJ/mol), because, based on the analysis of Jencks (*53*) and Murray and Verdonk (*54*) applied to galectin-ligand interaction (*33*), the relatively large free energy cost due to loss of rigid body translational and rotational entropy when two particles become one is overcome by the many ligand−protein interactions in the canonical galectin binding site (C−D in Figure 1). One possible source of these small changes in free energy of binding is interactions between added ligand fragments with an added (extended) binding sites on the protein, and a variety of interaction types involving single functional groups are sufficient to cause changes in free energy of sufficient magnitude (*55*). Modeling of compound **2** (Figure 5) shows that when one lactose residue binds the canonical galectin binding site (C−D in Figure 1), the linker and the other lactose residue can reach far enough to provide interactions with other parts of the CRD. Although we cannot identify the exact nature of these interactions, they are expected to need some degree of stereochemical fit, which predicts that some multivalent ligands would give enhanced affinity (an apparent "cluster effect") whereas others would not. This was indeed the case because other synthetic divalent−tetravalent saccharides (*43*, *56*) and the biantennary N-glycan (Table 1) did not show any "cluster effect" with galectin-1 in solution even if both arms were accessible for binding (*45*). The stereochemical fit in the secondary site would also depend on the galectin, and in fact galectins-3, -4, and -7 and the N-CRDs of galectins-8 and -9 did not show any cluster effect with compound **2** (*27*). Alternative and/or secondary potentially affinity enhancing binding sites on galectin-1 for complex plant polysaccharides have also been indicated by chemical shift mapping and other careful NMR experiments (*57*, *58*).

Other sources of the enhanced binding affinity due to an added ligand fragment, but not caused by interactions in an added protein site, include effects on properties of the ligand itself, such as solvatization, altered mobility of the primary interacting part, and maybe others (*55*). In these cases the enhanced affinity is not expected to depend as much on the stereochemical fit between the added ligand fragment and the protein and, hence, in the present case expected to be similar for different galectins. However, the size of the many different energy contributions to protein−ligand interactions is still not well understood, which is one reason why

they are hard to model even if the structure of a complex is known (*59*, *60*). One illustration of this is the recently recognized large contribution of ligand-induced increased mobility (providing beneficial conformational entropy) of galectin- 1 and galectin- 3 (*37*, *61*), and effects of ligand modifications on this could perhaps also cause altered affinity. A different type of cause for apparently enhanced affinity of a protein for a multivalent ligand is recapture of the protein on additional primary sites (*3*, *47*) as discussed regarding asialofetuin below.

Asialofetuin was analyzed as a commonly used multivalent model glycoprotein, albeit unnatural; it is a mixture of glycoforms (*46*), with on average nine galectin-1 binding sites (*47*). The results demonstrated the applicability of the FA assays and calculations in this system, even in the presence of galectin-1−ASF aggregates. When tested at low concentration and in the presence of excess ASF, the binding data were consistent with the presence of about 0.5−1 binding site per ASF molecule both for dHumGal-1 and for mHumGal-1, with low micromolar affinity (K_d ~3 and 10 μM, respectively). When tested at higher concentration, with the first site occupied, the data suggested about eight additional sites on average per ASF molecule, with a range of lower affinities. This suggests that dimerization of galectin-1 increases affinity for the first site by about the same factor (×3−5) as it contributes to the binding of surface coated glycans (*13*), but monovalent interactions also contribute since the affinities of both the dimeric and monomeric galectin-1s were much higher (×30−50) than for component saccharides such as the diantennary N-glycan and LacNAc. The mechanism of the dimer contribution may be cross-linking as has been suggested (*13*), but it may also be the newly recognized cooperativity (*37*) that will enhance binding to the first CRD in the dimer over the monomer by a factor of ~5 (Supporting Information Figure S8).

Our results for the binding of dHumGal-1 to ASF agreed with general aspects of published data: the average macroscopic affinity for ASF was similar (~3 vs 2 μM), and on average about nine galectin-1 binding sites per ASF molecule were found with decreasing microscopic affinities as total added galectin increased (*47*); at high galectin concentrations, galectin−ASF precipitates formed with ratios of 3 or higher (*48*−*50*). However, the details of the analyses and interpretations differ. Dam et al. (*47*) used isothermal titration calorimetry to analyze binding of ASF to an excess of galectin-1 (35 μM galectin-1 to which ASF was added in ~1 μM increments), i.e., the opposite of the present analysis. The calorimetric data were converted to concentrations of galectin−ASF complexes formed and further analyzed by Hill plots under the assumption that all nine binding sites on ASF had the same microscopic affinity, similar to LacNAc; the apparent increasing negative cooperativity of galectin binding to ASF was explained by decreasing availability of sites as more and more galectin molecules bound to one ASF molecule; based on the estimate that the last bound galectin would have the same affinity as LacNAc (K_d ~ 100 μM), and thus 50-fold lower than the macroscopic average (K_d ~ 2 μM), it was extrapolated that the first bound galectin would have a 50-fold higher affinity (K_d ~40 nM) as a result of a recapture effect to the multivalent ASF. Such high-affinity binding of the first galectin-1 to ASF was clearly not found in our analysis but should have been detected as much greater inhibitory potency of ASF when analyzed with low concentrations of galectin-1 (Table 2, Figure 6A). We favor an interpretation of our data and those of Dam et al., where the different galectin binding sites on ASF do not have the same microscopic affinity but instead differ based on the particular structural context of the binding site, both within the N-glycan and its peptide environment. In support of this interpretation we found that low salt conditions affected the sites differently, i.e., strongly decreased the binding to the low-affinity sites but did not affect binding to the high-affinity site on ASF or to the component saccharide MeLacNAc. The mechanisms leading to enhanced affinity of galectin-1 to the first site on ASF are not expected to be the same as leading to enhanced affinity of compound **2** over **1**, although they may very well include interactions in the same general area of the protein (site E in Figure 1). Added antennae of the N-glycan and parts of the protein (arrows in Figure 1) to which it is attached are easily close enough, which also makes it very unlikely that all of the LacNAc residues on ASF would have the same microscopic affinity for galectin-1. This does not rule out that the recapture effect may also be an important contribution to the enhanced affinity of galectin-1 for a highly multivalent ligand as ASF, but not to the large extent suggested by Dam et al. (*47*).

The surprisingly poor affinity of fetuin for galectin-1 gives further evidence for the importance of the specific structural context of galectin binding sites (Table 2, Figure 6D). Most of the LacNAc residues of fetuin are capped by 2−3 sialic acids (*46*) or uncapped and should be as good ligands for galectin-1 as LacNAc (*13*, *51*); only < 40% are capped by 2−6 sialic acid that would block galectin binding. Apparently, the high-affinity and many of the low-affinity galectin-1 binding sites found in ASF are hindered in fetuin by mechanisms other than 2−6 sialic acid.

We finally characterized the interaction of galectin-1 with human serum, since galectin-1 binds a selected set of human serum glycoproteins (mainly α-2 macroglobulin, IgM, and haptoglobin, Figure 8B), and the level of this binding is altered in cancer patient sera and has functional consequence when the glycoproteins are taken up by tissue cells.[2] Galectin-1 bound 20−40 μM high-affinity (K_d ~2−4 μM) sites on human serum proteins in a carbohydrate-dependent manner, which is at most only about 1/40−1/20 of the total of 800 μM N-glycans carried by human serum glycoproteins (*62*) and only about 1/8−1/4 of those with potential galectin binding sites (uncapped or NeuAcα2−3 capped LacNAc-residues; see Supporting Information Table S3 in ref *35*). Thus additional features of the binding site are needed for high-affinity galectin-1 binding. Further evidence for this is the affinity enhancement over the known component galectin binding saccharide moieties, MeLacNAc and the biantennary N-glycan (Table 1), of at least 30−50. In this case the affinity enhancement was the same for dHumGal-1 and mHumGal-1, demonstrating little contribution of galectin dimerization. The results with the C3S/N34D mutant suggested that high-affinity galectin-1 binding requires a third antenna on triantennary N-glycans, uncapped or capped by NeuAcα2−3, which is present at ~50 μM on human serum glycoproteins. Such trianatennary N-glycans are known to occur at specific sites on the three main galectin-1 binding serum glycoproteins, α-2-macroglobulin (*63*), IgM (*64*), and haptoglobin (*65*). However, representatives of the potential galectin-1-binding tri- and tetraantennary glycans found on serum glycoproteins bind galectin-1 with about equal affinity as the biantennary glycan tested in solution here (Table 1), when tested on a recently reported N-glycan array (*66*) and by frontal affinity chromatography (*38*, *67*). Therefore, additional interactions are most likely required, either with a special conformation of the N-glycan induced by the context of the glycoprotein or directly with the peptide part of the

glycoprotein which may come close enough to an extended binding site on the galectin CRD (Figure 1).

The different or lacking interactions of other galectins with serum glycoproteins provide additional evidence for selectivity determinants beyond binding available LacNAc residues. Galectin-3 binds a larger amount and wider range of serum glycoproteins than galectin-1, whereas galectins-2, -4, and -7 do not show any binding (*35*), despite the fact that they have similar affinity for LacNAc and the N-glycans of ASF as does galectin-1 (*47*). The mechanisms leading to enhanced affinity of galectin-1 for certain serum glycoproteins may not be exactly the same in each case and also not the same as those for compound **2** or ASF. As mentioned above, there are many mechanisms by which small added ligand interactions can cause increased affinities of the magnitude discussed here (*55*).

The binding of galectin-1 to carbohydrate-coated surfaces and cell surfaces has been analyzed in detail in a number of studies, e.g., ref *13*, and affinities (K_d = 2−5 μM) found in the same range as those found here for serum glycoproteins in solution. Although divalent binding was proposed to explain the higher affinity for surface-bound glycans compared to soluble glycans, there was only a small (*13*) or no difference (*39*) between dimeric galectin-1 and the monomeric mutant (same as used here). Thus, also in these cases, most of the affinity is provided by a single CRD perhaps by interaction of neighboring saccharides with a secondary weak binding site.

The estimated affinity of galectin-1 for serum glycoproteins is, as mentioned above, similar to its affinity for cell surfaces and clearly sufficient for it to be active at the concentrations inducing various functional effects on cells (*17*, *18*, *39*). Even if most of the ligand binding affinity of galectin-1 is provided by a single CRD, the dimerization enables cross-linking of ligands or surfaces. In other words, if both monomers of the galectin-1 dimer were required for high-affinity binding, the dimeric galectin would be functionally monovalent for that ligand. This would make many of the proposed cross-linking functions of galectin-1 difficult, for example, mediating cell surface interaction with other cells or external glycoproteins, cross-linking of cell surface receptors, and formation of lattices. The structure of galectin-1 (Figure 1) with each canonical binding site at opposite ends of the molecule, and pointing in opposite directions, may have been selected for because it limits divalent interaction with the same ligand. Instead, it seems likely that most binding affinity for a ligand is provided for by the interactions with a single CRD and that lectin dimerization permits cross-linking important for biological function (*6*, *7*).

ACKNOWLEDGMENT

The authors thank Barbro Kahl-Knutson for excellent laboratory assistance, Christopher Öberg for providing probes used for fluorescence anisotropy, and Michael Carlsson and Franck Touret for help with some galectin experiments and fruitful discussions.

SUPPORTING INFORMATION AVAILABLE

Characterization of dimeric and monomeric galectin-1 (text); characterization of monomeric rat galectin-1 (Figure S1); analysis of galectin-1 monomer−dimer equilibrium by fluorescence anisotropy (Figure S2); dynamic light scattering of dHumGal-1 and mHumGal-1 (Figure S3); sensitivity of galectins to oxidative inactivation (Figure S4); dynamic light scattering of asialofetuin with different concentrations of dHumGal-1 and mHumGal-1 (Figure S5); interaction between galectin-1s, **tdga-probe**, and MeLacNAc (Figure S6); interaction between galectin-1s, **FucLac-probe**, and MeLacNAc (Figure S7); interaction of galectin-1s with lactose (Figure S8); interaction of galectin-1s with the divalent compound **2** and its monovalent counterpart **1** (Figure S9); X-ray structure determination of rat galectin-1 (text); data collection and refinement statistics (Table S1); demonstration that ASF−galectin precipitates do not affect fluorescence intensity of the probes (Table S2); demonstration that ASF−galectin precipitates do not affect the fluorescence anisotropy and derived percent bound probe of the samples (Figure S10); different affinities of ASF for dHumGal-1 in low salt buffer compared to PBS (Table S3); analysis of galectin-1 stability in human serum (text); stability of galectin-1 mutants in human serum (Table S4); Hill plots of human galectin-1 binding to serum glycoproteins (Figure S11); interaction of rat galectin-1 with human serum glycoproteins (Figure S12); synthesis of fluorescent **tdga-probe** (text and Scheme S1). This material is available free of charge via the Internet at http://pubs.acs.org.

REFERENCES

1. Liu, F. T., and Rabinovich, G. A. (2005) Galectins as modulators of tumour progression. *Nat. Rev. Cancer 5*, 29–41.
2. Yang, R. Y., Rabinovich, G. A., and Liu, F. T. (2008) Galectins: structure, function and therapeutic potential. *Expert Rev. Mol. Med. 10*, e17.
3. Dam, T. K., and Brewer, C. F. (2008) Effects of clustered epitopes in multivalent ligand-receptor interactions. *Biochemistry 47*, 8470–8476.
4. Sacchettini, J. C., Baum, L. G., and Brewer, C. F. (2001) Multivalent protein-carbohydrate interactions. A new paradigm for supermolecular assembly and signal transduction. *Biochemistry 40*, 3009–3015.
5. Garner, O. B., and Baum, L. G. (2008) Galectin-glycan lattices regulate cell-surface glycoprotein organization and signalling. *Biochem. Soc. Trans. 36*, 1472–1477.
6. Lau, K. S., and Dennis, J. W. (2008) N-Glycans in cancer progression. *Glycobiology 18*, 750–760.
7. Lau, K. S., Partridge, E. A., Grigorian, A., Silvescu, C. I., Reinhold, V. N., Demetriou, M., and Dennis, J. W. (2007) Complex N-glycan number and degree of branching cooperate to regulate cell proliferation and differentiation. *Cell 129*, 123–134.
8. Delacour, D., Greb, C., Koch, A., Salomonsson, E., Leffler, H., Le Bivic, A., and Jacob, R. (2007) Apical sorting by galectin-3-dependent glycoprotein clustering. *Traffic 8*, 379–388.
9. Fortin, S., Le Mercier, M., Camby, I., Spiegl-Kreinecker, S., Berger, W., Lefranc, F., and Kiss, R. (2008) Galectin-1 is implicated in the protein kinase C epsilon/vimentin-controlled trafficking of integrin-beta1 in glioblastoma cells. *Brain Pathol. 20*, 39–49.
10. Cha, S. K., Ortega, B., Kurosu, H., Rosenblatt, K. P., Kuro, O. M., and Huang, C. L. (2008) Removal of sialic acid involving Klotho causes cell-surface retention of TRPV5 channel via binding to galectin-1. *Proc. Natl. Acad. Sci. U.S.A. 105*, 9805–9810.
11. Lee, R. T., and Lee, Y. C. (2000) Affinity enhancement by multivalent lectin-carbohydrate interaction. *Glycoconjugate J. 17*, 543–551.
12. Lundquist, J. J., and Toone, E. J. (2002) The cluster glycoside effect. *Chem. Rev. 102*, 555–578.
13. Leppanen, A., Stowell, S., Blixt, O., and Cummings, R. D. (2005) Dimeric galectin-1 binds with high affinity to alpha2,3-sialylated and non-sialylated terminal N-acetyllactosamine units on surface-bound extended glycans. *J. Biol. Chem. 280*, 5549–5562.
14. Ozaki, K., Lee, R. T., Lee, Y. C., and Kawasaki, T. (1995) The differences in structural specificity for recognition and binding between asialoglycoprotein receptors of liver and macrophages. *Glycoconjugate J. 12*, 268–274.
15. Collins, B. E., and Paulson, J. C. (2004) Cell surface biology mediated by low affinity multivalent protein-glycan interactions. *Curr. Opin. Chem. Biol. 8*, 617–625.
16. Mammen, M., Choi, S.-K., and Whitesides, G. M. (1998) Polyvalent interactions in biological systems: implications for design and use of multivalent ligands and inhibitors. *Angew. Chem., Int. Ed. 37*, 2754–2794.
17. Toscano, M. A., Bianco, G. A., Ilarregui, J. M., Croci, D. O., Correale, J., Hernandez, J. D., Zwirner, N. W., Poirier, F., Riley,

E. M., Baum, L. G., and Rabinovich, G. A. (2007) Differential glycosylation of TH1, TH2 and TH-17 effector cells selectively regulates susceptibility to cell death. *Nat. Immunol. 8*, 825–834.
18. Blois, S. M., Ilarregui, J. M., Tometten, M., Garcia, M., Orsal, A. S., Cordo-Russo, R., Toscano, M. A., Bianco, G. A., Kobelt, P., Handjiski, B., Tirado, I., Markert, U. R., Klapp, B. F., Poirier, F., Szekeres-Bartho, J., Rabinovich, G. A., and Arck, P. C. (2007) A pivotal role for galectin-1 in fetomaternal tolerance. *Nat. Med. 13*, 1450–1457.
19. Thijssen, V. L., Poirier, F., Baum, L. G., and Griffioen, A. W. (2007) Galectins in the tumor endothelium: opportunities for combined cancer therapy. *Blood 110*, 2819–2827.
20. Wu, M. H., Hong, T. M., Cheng, H. W., Pan, S. H., Liang, Y. R., Hong, H. C., Chiang, W. F., Wong, T. Y., Shieh, D. B., Shiau, A. L., Jin, Y. T., and Chen, Y. L. (2009) Galectin-1-mediated tumor invasion and metastasis, up-regulated matrix metalloproteinase expression, and reorganized actin cytoskeletons. *Mol. Cancer Res. 7*, 311–318.
21. Perone, M. J., Bertera, S., Shufesky, W. J., Divito, S. J., Montecalvo, A., Mathers, A. R., Larregina, A. T., Pang, M., Seth, N., Wucherpfennig, K. W., Trucco, M., Baum, L. G., and Morelli, A. E. (2009) Suppression of autoimmune diabetes by soluble galectin-1. *J. Immunol. 182*, 2641–2653.
22. Pohl, N. L., and Kiessling, L. L. (1999) Scope of multivalent ligand function: lactose-bearing neoglycopolymers by ring-opening metathesis polymerization, *Synthesis*.
23. Andre, S., Frisch, B., Kaltner, H., Desouza, D. L., Schuber, F., and Gabius, H. J. (2000) Lectin-mediated drug targeting: selection of valency, sugar type (Gal/Lac), and spacer length for cluster glycosides as parameters to distinguish ligand binding to C-type asialoglycoprotein receptors and galectins. *Pharm. Res. 17*, 985–990.
24. Vrasidas, I., Andre, S., Valentini, P., Bock, C., Lensch, M., Kaltner, H., Liskamp, R. M., Gabius, H. J., and Pieters, R. J. (2003) Rigidified multivalent lactose molecules and their interactions with mammalian galectins: a route to selective inhibitors. *Org. Biomol. Chem. 1*, 803–810.
25. Andre, S., Liu, B., Gabius, H. J., and Roy, R. (2003) First demonstration of differential inhibition of lectin binding by synthetic tri- and tetravalent glycoclusters from cross-coupling of rigidified 2-propynyl lactoside. *Org. Biomol. Chem. 1*, 3909–3916.
26. Wu, A. M., Wu, J. H., Liu, J. H., Singh, T., Andre, S., Kaltner, H., and Gabius, H. J. (2004) Effects of polyvalency of glycotopes and natural modifications of human blood group ABH/Lewis sugars at the Galbeta1-terminated core saccharides on the binding of domain-I of recombinant tandem-repeat-type galectin-4 from rat gastrointestinal tract (G4-N). *Biochimie 86*, 317–326.
27. Tejler, J., Tullberg, E., Frejd, T., Leffler, H., and Nilsson, U. J. (2006) Synthesis of multivalent lactose derivatives by 1,3-dipolar cycloadditions: selective galectin-1 inhibition. *Carbohydr. Res. 341*, 1353–1362.
28. Morris, S., Ahmad, N., Andre, S., Kaltner, H., Gabius, H. J., Brenowitz, M., and Brewer, F. (2004) Quaternary solution structures of galectins-1, -3, and -7. *Glycobiology 14*, 293–300.
29. Leffler, H., Carlsson, S., Hedlund, M., Qian, Y., and Poirier, F. (2004) Introduction to galectins. *Glycoconjugate J. 19*, 433–440.
30. Dias-Baruffi, M., Zhu, H., Cho, M., Karmakar, S., McEver, R. P., and Cummings, R. D. (2003) Dimeric galectin-1 induces surface exposure of phosphatidylserine and phagocytic recognition of leukocytes without inducing apoptosis. *J. Biol. Chem. 278*, 41282–41293.
31. Hirabayashi, J., and Kasai, K. (1991) Effect of amino acid substitution by sited-directed mutagenesis on the carbohydrate recognition and stability of human 14-kDa beta-galactoside-binding lectin. *J. Biol. Chem. 266*, 23648–23653.
32. Cooper, D. N., Massa, S. M., and Barondes, S. H. (1991) Endogenous muscle lectin inhibits myoblast adhesion to laminin. *J. Cell Biol. 115*, 1437–1448.
33. Carlsson, S., Oberg, C. T., Carlsson, M. C., Sundin, A., Nilsson, U. J., Smith, D., Cummings, R. D., Almkvist, J., Karlsson, A., and Leffler, H. (2007) Affinity of galectin-8 and its carbohydrate recognition domains for ligands in solution and at the cell surface. *Glycobiology 17*, 663–676.
34. Sorme, P., Kahl-Knutsson, B., Huflejt, M., Nilsson, U. J., and Leffler, H. (2004) Fluorescence polarization as an analytical tool to evaluate galectin-ligand interactions. *Anal. Biochem. 334*, 36–47.
35. Cederfur, C., Salomonsson, E., Nilsson, J., Halim, A., Oberg, C. T., Larson, G., Nilsson, U. J., and Leffler, H. (2008) Different affinity of galectins for human serum glycoproteins: galectin-3 binds many protease inhibitors and acute phase proteins. *Glycobiology 18*, 384–394.
36. Cederfur, C. (2008) Galectin binding proteins in serum and bronchoalveolar lavage, Ph.D. Thesis, Lund University, H. Leffler, supervisor.
37. Nesmelova, I. V., Ermakova, E., Daragan, V. A., Pang, M., Menendez, M., Lagartera, L., Solis, D., Baum, L. G., and Mayo, K. H. (2010) Lactose binding to galectin-1 modulates structural dynamics, increases conformational entropy, and occurs with apparent negative cooperativity. *J. Mol. Biol. 397*, 1209–1230.
38. Nishi, N., Abe, A., Iwaki, J., Yoshida, H., Itoh, A., Shoji, H., Kamitori, S., Hirabayashi, J., and Nakamura, T. (2008) Functional and structural bases of a cysteine-less mutant as a long-lasting substitute for galectin-1. *Glycobiology 18*, 1065–1073.
39. Stowell, S. R., Cho, M., Feasley, C. L., Arthur, C. M., Song, X., Colucci, J. K., Karmakar, S., Mehta, P., Dias-Baruffi, M., McEver, R. P., and Cummings, R. D. (2009) Ligand reduces galectin-1 sensitivity to oxidative inactivation by enhancing dimer formation. *J. Biol. Chem. 284*, 4989–4999.
40. Cumpstey, I., Salomonsson, E., Sundin, A., Leffler, H., and Nilsson, U. J. (2008) Double affinity amplification of galectin-ligand interactions through arginine-arene interactions: synthetic, thermodynamic, and computational studies with aromatic diamido thiodigalactosides. *Chemistry 14*, 4233–4245.
41. Stannard, K. A., Collins, P., Ito, K., Sullivan, E. M., Scott, S., Gabutero, E., Low, P., Nilsson, U. J., Leffler, H., Blanchard, H., and Ralph, S. J. (2010) Galectin inhibitory disaccharides promote tumour immunity in a breast cancer model, *Cancer Lett*., September 6 (Epub ahead of print).
42. Cumpstey, I., Carlsson, S., Leffler, H., and Nilsson, U. J. (2005) Synthesis of a phenyl thio-beta-D-galactopyranoside library from 1, 5-difluoro-2,4-dinitrobenzene: discovery of efficient and selective monosaccharide inhibitors of galectin-7. *Org. Biomol. Chem. 3*, 1922–1932.
43. Gouin, S. G., Fernández, J. M. G., Vanquelef, E., Dupradeau, F.-Y., Salomonsson, E., Leffler, H., Ortega-Muñoz, M., Nilsson, U. J., and Kovensky, J. (2010) Multimeric lactoside "click clusters" as tools to investigate the effect of linker length in specific interactions with peanut lectin, galectin-1, and -3, *ChemBioChem* 11, 1430−1442.
44. Lopez-Lucendo, M. F., Solis, D., Andre, S., Hirabayashi, J., Kasai, K., Kaltner, H., Gabius, H. J., and Romero, A. (2004) Growth-regulatory human galectin-1: crystallographic characterisation of the structural changes induced by single-site mutations and their impact on the thermodynamics of ligand binding. *J. Mol. Biol. 343*, 957–970.
45. Bourne, Y., Bolgiano, B., Liao, D. I., Strecker, G., Cantau, P., Herzberg, O., Feizi, T., and Cambillau, C. (1994) Crosslinking of mammalian lectin (galectin-1) by complex biantennary saccharides. *Nat. Struct. Biol. 1*, 863–870.
46. Green, E. D., Adelt, G., Baenziger, J. U., Wilson, S., and Van Halbeek, H. (1988) The asparagine-linked oligosaccharides on bovine fetuin. Structural analysis of N-glycanase-released oligosaccharides by 500-megahertz ^{1}H NMR spectroscopy. *J. Biol. Chem. 263*, 18253–18268.
47. Dam, T. K., Gabius, H. J., Andre, S., Kaltner, H., Lensch, M., and Brewer, C. F. (2005) Galectins bind to the multivalent glycoprotein asialofetuin with enhanced affinities and a gradient of decreasing binding constants. *Biochemistry 44*, 12564–12571.
48. Gupta, D., and Brewer, C. F. (1994) Homogeneous aggregation of the 14-kDa beta-galactoside specific vertebrate lectin complex with asialofetuin in mixed systems. *Biochemistry 33*, 5526–5530.
49. Gupta, D., Kaltner, H., Dong, X., Gabius, H. J., and Brewer, C. F. (1996) Comparative cross-linking activities of lactose-specific plant and animal lectins and a natural lactose-binding immunoglobulin G fraction from human serum with asialofetuin. *Glycobiology 6*, 843–849.
50. Mandal, D. K., and Brewer, C. F. (1992) Cross-linking activity of the 14-kilodalton beta-galactoside-specific vertebrate lectin with asialofetuin: comparison with several galactose-specific plant lectins. *Biochemistry 31*, 8465–8472.
51. Stowell, S. R., Arthur, C. M., Mehta, P., Slanina, K. A., Blixt, O., Leffler, H., Smith, D. F., and Cummings, R. D. (2008) Galectin-1, -2, and -3 exhibit differential recognition of sialylated glycans and blood group antigens. *J. Biol. Chem. 283*, 10109–10123.
52. Houzelstein, D., Goncalves, I. R., Fadden, A. J., Sidhu, S. S., Cooper, D. N., Drickamer, K., Leffler, H., and Poirier, F. (2004) Phylogenetic analysis of the vertebrate galectin family. *Mol. Biol. Evol. 21*, 1177–1187.
53. Jencks, W. P. (1981) On the attribution and additivity of binding energies. *Proc. Natl. Acad. Sci. U.S.A. 78*, 4046–4050.
54. Murray, C. W., and Verdonk, M. L. (2002) The consequences of translational and rotational entropy lost by small molecules on binding to proteins. *J. Comput.-Aided Mol. Des. V16*, 741–753.
55. Bissantz, C., Kuhn, B., and Stahl, M. (2010) A medicinal chemist's guide to molecular interactions. *J. Med. Chem. 53*, 5061–5084.

56. Ahmad, N., Gabius, H. J., Sabesan, S., Oscarson, S., and Brewer, C. F. (2004) Thermodynamic binding studies of bivalent oligosaccharides to galectin-1, galectin-3, and the carbohydrate recognition domain of galectin-3. *Glycobiology 14*, 817–825.
57. Miller, M. C., Klyosov, A., and Mayo, K. H. (2009) The alpha-galactomannan Davanat binds galectin-1 at a site different from the conventional galectin carbohydrate binding domain. *Glycobiology 19*, 1034–1045.
58. Miller, M. C., Nesmelova, I. V., Platt, D., Klyosov, A., and Mayo, K. H. (2009) The carbohydrate-binding domain on galectin-1 is more extensive for a complex glycan than for simple saccharides: implications for galectin-glycan interactions at the cell surface. *Biochem. J. 421*, 211–221.
59. Gohlke, H., and Klebe, G. (2002) Approaches to the description and prediction of the binding affinity of small-molecule ligands to macromolecular receptors. *Angew. Chem., Int. Ed. Engl. 41*, 2644–2676.
60. Weis, A., Katebzadeh, K., Soderhjelm, P., Nilsson, I., and Ryde, U. (2006) Ligand affinities predicted with the MM/PBSA method: dependence on the simulation method and the force field. *J. Med. Chem. 49*, 6596–6606.
61. Diehl, C., Engström, O., Delaine, T., Hakansson, M., Genheden, S., Modig, K., Leffler, H., Ryde, U., Nilsson, U. J., and Akke, M. (2010) Protein flexibility and conformational entropy in ligand design targeting the carbohydrate recognition domain of galectin-3, *J. Am. Chem. Soc*., September 28 (Epub ahead of print).
62. Kita, Y., Miura, Y., Furukawa, J., Nakano, M., Shinohara, Y., Ohno, M., Takimoto, A., and Nishimura, S. (2007) Quantitative glycomics of human whole serum glycoproteins based on the standardized protocol for liberating N-glycans. *Mol. Cell Proteomics 6*, 1437–1445.
63. Arnold, J. N., Wallis, R., Willis, A. C., Harvey, D. J., Royle, L., Dwek, R. A., Rudd, P. M., and Sim, R. B. (2006) Interaction of mannan binding lectin with alpha2 macroglobulin via exposed oligomannose glycans: a conserved feature of the thiol ester protein family? *J. Biol. Chem. 281*, 6955–6963.
64. Arnold, J. N., Wormald, M. R., Suter, D. M., Radcliffe, C. M., Harvey, D. J., Dwek, R. A., Rudd, P. M., and Sim, R. B. (2005) Human serum IgM glycosylation: identification of glycoforms that can bind to mannan-binding lectin. *J. Biol. Chem. 280*, 29080–29087.
65. Nakano, M., Nakagawa, T., Ito, T., Kitada, T., Hijioka, T., Kasahara, A., Tajiri, M., Wada, Y., Taniguchi, N., and Miyoshi, E. (2008) Site-specific analysis of N-glycans on haptoglobin in sera of patients with pancreatic cancer: a novel approach for the development of tumor markers. *Int. J. Cancer 122*, 2301–2309.
66. Song, X., Xia, B., Stowell, S. R., Lasanajak, Y., Smith, D. F., and Cummings, R. D. (2009) Novel fluorescent glycan microarray strategy reveals ligands for galectins. *Chem. Biol. 16*, 36–47.
67. Hirabayashi, J., Hashidate, T., Arata, Y., Nishi, N., Nakamura, T., Hirashima, M., Urashima, T., Oka, T., Futai, M., Muller, W. E., Yagi, F., and Kasai, K. (2002) Oligosaccharide specificity of galectins: a search by frontal affinity chromatography. *Biochim. Biophys. Acta 1572*, 232–254.